Hindawi
Mathematical Problems in Engineering
Volume 2021, Article ID 4862451, 10 pages
https://doi.org/10.1155/2021/4862451

Research Article

Research on Continuous Wave Electromagnetic Effect in Swept Frequency Radar

Xue Du, Guanghui Wei, Hongze Zhao, and Xiaodong Pan

National Key Laboratory on Electromagnetic Environmental Effects, Shijiazhuang Campus of Army Engineering University, Shijiazhuang 050003, China

Correspondence should be addressed to Guanghui Wei; wei-guanghui@sohu.com

Received 22 June 2021; Revised 15 October 2021; Accepted 15 December 2021; Published 31 December 2021

Academic Editor: Isabella Torcicollo

In order to establish the prediction model of radar equipment in multisource complex electromagnetic environment, the blocking effect and false alarm interference effect caused by single-frequency CW (continuous wave) electromagnetic interference on typical radar equipment are studied. Taking a certain sweep radar as the research object, the equivalent injection test of EMI (electromagnetic interference) is carried out. Based on the theory of radar front door coupling, the interference mechanism of EMI to radar receiver RF front end is revealed, and the variation law of blocking target and false alarm target level is analyzed. The results show that, under the single-frequency CW-EMI, the target echo level decreases with the increase of the interference field strength, and the false alarm level increases with the increase of the interference field strength. The blocking jamming sensitive bandwidth is about $f_0 \pm 200$ MHz, and the false alarm jamming sensitive bandwidth is about $f_0 \pm 80$ MHz.

1. Introduction

With the continuous improvement of information integration of weapon equipment, the battlefield electromagnetic environment is becoming increasingly complex and harsh. Whether the information equipment has good adaptability to electromagnetic environment has become a decisive factor in battlefield intelligence, reconnaissance, and monitoring, which directly affects the operational efficiency of frequency equipment and even affects the success or failure of the war [1–5]. Today, with the rapid development of information technology, many countries have invested a lot of energy to research direction of unmanned battlefields, in order to occupy an active position in the information battlefield, maximize the human-computer interaction performance of the unmanned combat systems, and improve the combat capability of the team [6, 7].

Radar plays an important role in unmanned combat systems. It is widely used in battlefield reconnaissance, target surveillance, aiming, and other operational scenarios, its working process is vulnerable to external electromagnetic interference, and its regular work environment may include high-power transmitters and high-sensitivity receiver; the existence of different working frequency bands leads to the concentration of space electromagnetic energy density, which affects the performance combat effectiveness of radar [8–11]. Therefore, it is of great military significance to study the law of electromagnetic interference effect of radar equipment. There are also a lot of interference studies on frequency receiver at home and abroad. Elena-Simona Lohan studied the influence of CW interference on the receiver E1 signal and proved that the high-power CW interference reduced the E1 reception performance of the navigation receiver [12]. Literature [13, 14] studied the effect of electromagnetic radiation on communication radio stations and concluded that under the action of electromagnetic radiation, the radio stations would have effects such as increased bit error rate, decreased voice quality and even communication interruption, abnormal display, and restart. Among them, the first two effects are caused by the large signal blocking caused by the interference signal entering the radio frequency (RF) front end through the device antenna, which belongs to "front door" coupling. Display abnormalities, restarts, and other effects are caused by "backdoor"

coupling [15, 16]. Chen Yazhou's team of Army Engineering University studied the influence of electromagnetic field on low-noise amplifier in RF front-end circuit of a data link receiver and analyzed the damage mechanism of strong electromagnetic field on sensitive devices through electromagnetic irradiation and injection amplification [17]. Literature [18–20] introduced the test method that directional injection of differential mode can replace the electromagnetic radiation equivalent. Literature [14] carried out CW interference irradiation and injection experiments for a certain GNSS (Global Navigation Satellite System) receiver and obtained the sensitive frequency band of the receiver under interference. On this basis, the electromagnetic protection reinforcement method is proposed according to the weak link of the satellite navigation terminal electromagnetic protection [21]. Mazzochette proposed coherent sidelobe chancellors, sidelobe blanker, and prediction filters to reduce EMI [22]. Manda et al. studied the performance of polyphase sequences using cyclic algorithm pruned analyzed against EMI suppression [23]. Mohsen Eslami proposed a new RFI mitigation algorithm based on inverse temporal windowing and complex empirical mode decomposition (CEMD) [24]. Yu et al. applied the noise subspace projection operation to suppress the mainlobe interference signals received by multiple node radars [25]. Compared with the research on information jamming, the research on radar receiver is relatively less.

This study takes a certain frequency sweep radar as the research object, treats the tested radar as a "black box," based on the front door coupling theory of electromagnetic interference, carries out the EMI effect test by using the equivalent injection method from the radar RF front end, focusses on the suppression effect of single-frequency CW-EMI on radar useful signal and the generation of false target signal, and lays a foundation for further mechanism research and adaptability evaluation of radar equipment in multifrequency and multisource complex electromagnetic environment.

2. Interference Mechanism Analysis

2.1. Front Door Coupling Theory. The electromagnetic energy interference affects the radar equipment mainly through the "front door" coupling and "back door" coupling approaches [1]. The front door coupling mainly means that the electromagnetic energy is linearly coupled to the equipment system through the target antenna, transmission line, and so on, destroying the electronic equipment of the RF front end of the receiver. Backdoor coupling mainly refers to the electromagnetic energy coupling to the system through holes and slits to interfere with the electronic devices in the equipment [25, 26]. In this study, the continuous wave electromagnetic effect of a swept frequency radar is studied. Each unit in the equipment is independently shielded. The electromagnetic energy is mainly coupled to the RF front end through the receiving antenna, so the front door coupling effect is regarded as the focus of protection. Considering only the front door coupling path, the schematic diagram of radar electromagnetic interference is shown in Figure 1.

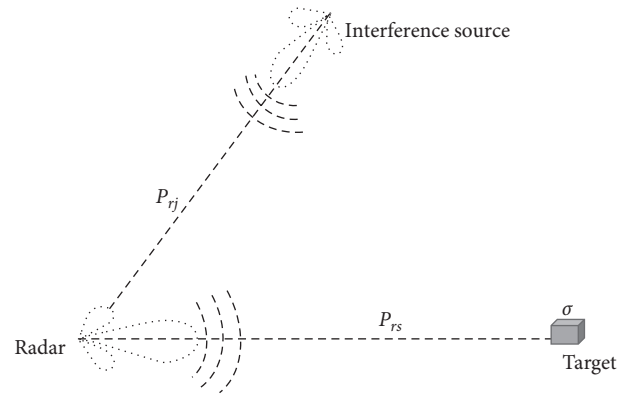

Figure 1: The schematic diagram of radar electromagnetic interference.

The power of the target echo signal received by the radar receiving antenna is as follows:

$$P_{rs} = \frac{P_t G_t \sigma A}{\left(4\pi R_t^2\right)^2 L_R} = \frac{P_t G_t^2 \sigma \lambda^2}{(4\pi)^3 R_t^4 L_R}, \tag{1}$$

where P_t is the radar transmitting power, G_t is the gain of the radar antenna, σ is the target radar cross section, A is the effective area of the radar antenna, R_t is the target radar range, and L_R is the radar system loss.

The power of the interference signal received by the radar is [2, 3]

$$P_{rj} = \frac{P_j G_j A' r_j}{4\pi R_t^2 L_j} = \frac{P_j G_j G_t' \lambda^2 r_j}{(4\pi)^2 R_j^2 L_j}, \tag{2}$$

where P_j is the interference power, G_j is the jamming antenna gain, R_j is the distance between jammer and radar, r_j is the polarization coefficient of jamming signal to the radar antenna, $A\prime$ is the effective area of the radar antenna in jammer direction, and G_t' is the corresponding gain of the radar antenna.

According to the power criterion, when $P_{rj}/P_{rs} \geq K_j$, the radar is effectively jammed.

2.2. Analysis of Radar Working Principle. The radar echo signal is amplified, filtered, and converted down. After that, the acquisition module collects the data of two channels, namely, in phase and orthogonal, and then the signal is processed and imaged through the data processing module. The block diagram of a typical radar receiving system is shown in Figure 2.

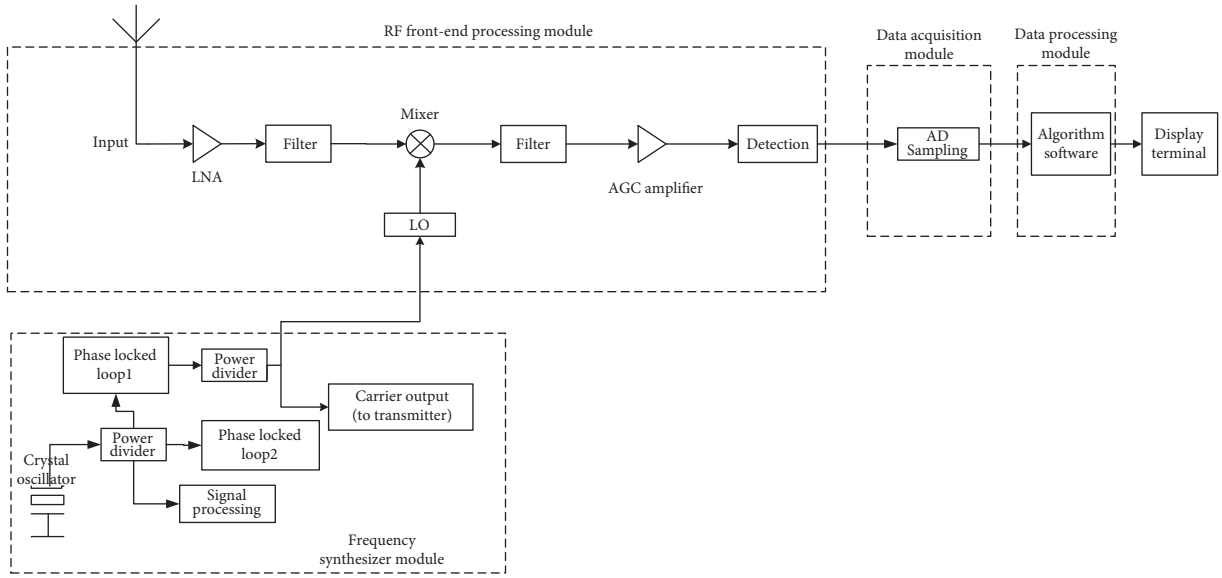

Figure 2: Block diagram of radar receiving system.

The RF front-end processing module is mainly composed of LNA (low-noise amplifier), mixer, filter, and so on. The electromagnetic energy received by the antenna is first coupled to the RF front end. Therefore, it is essential for the antenna system whether the interference signal can be filtered effectively in the RF front end. Without considering the internal circuit processing module of the RF front end, when the tested radar is processed as a "black box," the radar echo signal $u_s(t)$ and jamming signal $u_j(t)$ received by the receiver are, respectively, as follows:

$$u_s(t) = U_s \cos\left(\omega_s(t-\tau) + \varphi_s\right), \tag{3}$$

$$u_j(t) = U_j \cos\left(\omega_j t + \varphi_j\right), \tag{4}$$

where U_s and U_j represent the amplitude of useful signal and interference signal, respectively, ω_s and ω_j represent the angular frequency of useful signal and interference signal, respectively, and φ_s and φ_j represent the initial phase of useful signal and interference signal, respectively.

The antenna receives the signal from the RF front end:

$$u_1(t) = u_s(t) + u_j(t). \tag{5}$$

The frequency response of the filter can be expressed by a time-invariant filter with impulse response $h(t)$ [27], and then, the interference signals after filtering are $u_j'(t) = u_j(t) * h(t)$. So the input signal is expressed as follows after LNA and filter:

$$u_2(t) = k_s u_s'(t) + k_j u_j'(t), \tag{6}$$

where k_s and k_j are the magnification of the LNA.

Assume that the LO (local oscillator) signal is

$$u_l = U_L \cos\omega_l t, \tag{7}$$

where U_L is the amplitude of the LO signal and ω_l is the frequency of the LO signal.

Under ideal conditions, the receiver is in a linear working state, and the radar echo signal is obtained after mixing and low-pass filtering:

$$\begin{aligned} u_3(t) &= u_2(t) \cdot u_l(t) \\ &= \left[k_s u_s'(t) + k_j u_j'(t)\right] \cdot U_L \cos\omega_l t \\ &= \frac{1}{2} k_s U_s U_L \cos\left((\omega_s - \omega_l)t + \varphi_s - \omega_s \tau\right) + \frac{1}{2} k_j U_j U_L \cos\left(\left(\omega_j - \omega_l\right)t + \varphi_j\right). \end{aligned} \tag{8}$$

Before data sampling, the useful signal and interference signal are as follows:

$$u_{s1}(t) = \frac{1}{2}k_s U_s U_L \cos\left((\omega_s - \omega_l)t + \varphi_s - \omega_s \tau\right),$$
$$u_{j1}(t) = \frac{1}{2}k_j U_j U_L \cos\left(\left(\omega_j - \omega_l\right)t + \varphi_j\right). \tag{9}$$

When $((\omega_j - \omega_l)t + \varphi_j) \approx ((\omega_s - \omega_l)t + \varphi_s - \omega_s \tau)$, the receiver will misjudge the jamming signal for useful signal processing, resulting in a false target response. This phenomenon is defined as false alarm jamming, the phase of false alarm jamming signal is $((\omega_j - \omega_l)t + \varphi_j) \propto t$, and the distance of false alarm jamming is random.

The gain of useful signal and false alarm signal is as follows:

$$G_{s1}(t) = \frac{1}{2}k_s U_L,$$
$$G_{j1}(t) = \frac{1}{2}k_j U_L. \tag{10}$$

From equation (10), it can be seen that the gain of useful signal and false alarm signal is related to the amplitude of the LO. When the system is in a linear stage, useful signal and false alarm signal are linearly amplified.

When the input signal $u_1(t)$ is large, the receiver RF front end produces nonlinear distortion, and the power series analysis method is used for analysis [4]. When the input signal is equation (5), the output signal is

$$u_2'(t) = a_0 + a_1 u_1(t) + a_2 u_1^2(t) + a_3 u_1^3(t), \tag{11}$$

where $a_i\,(i = 0, 1, 2\ldots)$ is the nonlinear coefficient related to the circuit characteristics. After mixing and low-pass filtering, the signal is obtained as follows:

$$u_3(t) = u_2'(t) \cdot u_l(t). \tag{12}$$

According to the formulas (3)~(5), (7), and (11)~(12), the useful signal and false alarm signal components are as follows:

$$u_{s2}(t) = \left[a_1 + \frac{3}{2}a_3 U_j^2 + \frac{3}{4}a_3 U_s^2(t)\right] U_s U_L(t) \cos\left[(\omega_s - \omega_L)t - \omega_s \tau + \varphi_s\right],$$
$$u_{j2}(t) = \left[a_1 + \frac{3}{4}a_3 U_j^2 + \frac{3}{2}a_3 U_s^2(t)\right] U_j U_L \cos\left[\left(\omega_j - \omega_L\right)t + \varphi_j\right]. \tag{13}$$

The gain of useful signal and false alarm signal is as follows:

$$G_{s2}(t) = \left[a_1 + \frac{3}{2}a_3 U_j^2 + \frac{3}{4}a_3 U_s^2(t)\right] U_L(t) \cos\left[(\omega_s - \omega_L)t - \omega_s \tau + \varphi_s\right],$$
$$G_{j2}(t) = \left[a_1 + \frac{3}{4}a_3 U_j^2 + \frac{3}{2}a_3 U_s^2(t)\right] U_L \cos\left[\left(\omega_j - \omega_L\right)t + \varphi_j\right]. \tag{14}$$

When the input signal increases, the system will produce nonlinear distortion; and the gain of radar detection real target level decreases with the increase of the input signal, and the decrease increases gradually, resulting in blocking interference. The false alarm level continued to rise, but the increase rate decreased.

3. Interference Effect Test

3.1. Experimental Design of Interference Effect. In order to accurately evaluate the CW electromagnetic interference effect of radar frequency equipment, the electromagnetic radiation method was used to simulate the complex electromagnetic environment in [5]; however, the position of the amplifier is not considered in the simulation of strong electromagnetic field, and if the distance between the amplifier and the target antenna is small, it will cause interference to the receiving antenna. If the distance is large, the coaxial line attenuation is too large and the error of the test results is too large. Therefore, based on the principle of limited target, combined with GJB8848-2016 [28], this study adopts the equivalent method of differential mode injection instead of electromagnetic radiation test. On the one hand, it is convenient to analyze the coupling path of in-band interference in the receiver, and on the other hand, it can eliminate the influence of external electromagnetic environment on the test. As the simplest form of interference, single-frequency CW-EMI can reflect the basic properties of frequency equipment sensitive to different frequencies of electromagnetic radiation and reveal the basic law of electromagnetic interference effect.

Firstly, the CW electromagnetic effect test platform of radar equipment is constructed, and the test configuration diagram is shown in Figure 3 [29]. It consists of five parts: electromagnetic injection jamming system, signal injection area, data processing area, test radar, and target antenna. The microwave signal source, the microwave power amplifier, and injection module are connected by high-frequency coaxial cable. In order to reduce the influence of microwave power amplifier noise and ensure the smooth coupling of high-power working signal to the radar RF front end, the double-directional coupler is serially connected to the 30 dB fixed attenuator. The signal source generated interference signal and is coupled to the injection module through the microwave power amplifier, dual directional coupler, and attenuator to simulate the working state of the radiation system [29]. The radar processing terminal is connected to the monitoring computer through a network cable, and the working state of the radar can be read from the monitoring software of the display terminal. The field test is shown in Figure 4.

3.2. Experiment on the Interference Effect of Single-Frequency CW. The tested radar is a certain type of sweep frequency radar, which has the function of static target ranging, and its working frequency is $f_0 \pm 100$ MHz (f_0 is the center frequency). Combined with GJB8848-2016, typical interference frequency points were selected, namely, $\Delta f = \pm 30$ MHz, ± 60 MHz, ± 90 MHz, and 0 MHz [29]. By adjusting the frequency and signal strength of the microwave signal generator, the variation relationship between the radar

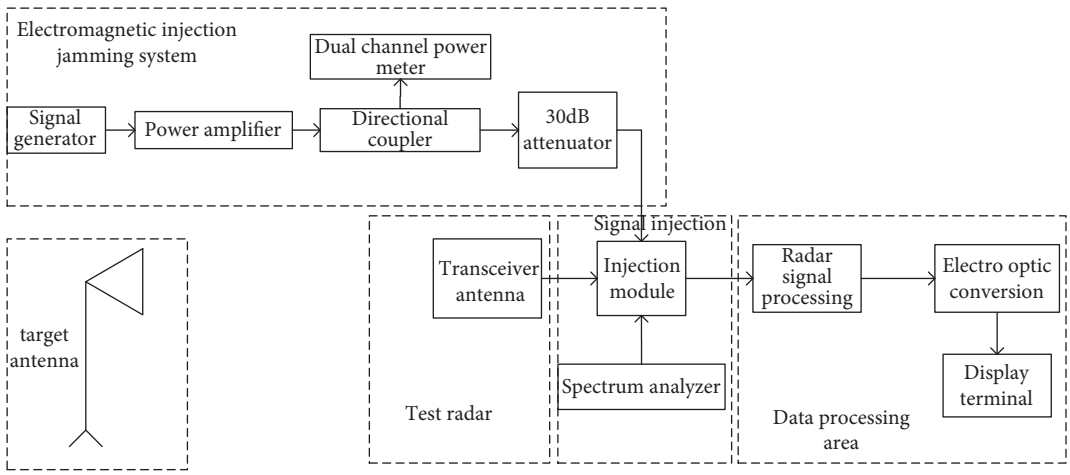

Figure 3: Configuration diagram of electromagnetic interference effect test.

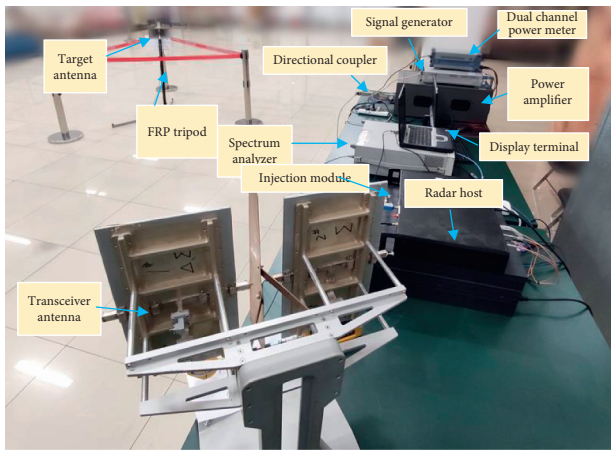

Figure 4: Field test chart.

target echo level and the interference field strength is established as shown in Figure 5.

It can be seen from Figure 5 that under different interference frequency offsets, the change law of the target echo level with interference field intensity is approximately consistent and the echo level decreases with the increase of interference field intensity.

When the interference field strength is between −35 dBV/m and −25 dBV/m, the tested radar works in the linear region, and the level is almost stable, which indicates that the useful signal gain is constant. With the increase of the interference field strength, that is, the interference field strength is between −25 dBV/m and −15 dBV/m, the RF front end produces nonlinear distortion, and the useful signal gain begins to decline. When the interference field strength increases to a certain extent (−20 dBV/m), the target echo level compression increases approximately linearly with the increase of the interference field strength.

The experiment uses the injection method, under the conditions of existing power amplifier and attenuator, and the useful signal cannot be completely blocked. Theoretically, the curve trend should be as shown in Figure 6.

The above ordinate is dBmV as the unit. If the ordinate is mV, the internal change trend is as shown in Figure 7.

When the input signal is weak, the useful signal gain is constant, $G_{s2}(t) = a_1 U_L$, and the system works in the linear region, so the target level is less suppressed and changes gently. When the input signal increases gradually, the system produces nonlinear distortion. At this time, the fundamental component of the useful signal decreases, the gain decreases gradually, and the target level decreases approximately linearly with the increase of the interference intensity. When the interference signal is too large, the system produces sudden nonlinear distortion, and the useful signal is completely blocked.

In this study, without considering the internal circuit processing module of the RF front end, the tested radar is treated as a "black box," the electromagnetic interference effect test results are obtained, and the results are summarized and analyzed.

In addition, when the interference frequency offset is close to the edge of the equipment under test ($\Delta f = 90$ MHz) and when the interference field strength increases to −5 dBV/m, the level turns. It is analyzed that the reason for this phenomenon may be that the input signal amplification ratio of the nondevices in the RF front end changes under the frequency offset and the interference field intensity.

Using the same test method, the relationship between the false alarm level and the interference field strength is obtained, as shown in Figure 8.

It can be seen from Figure 8 that

(1) Under different interference frequency offsets, the false alarm target level increases first and then slows down with the increase of interference intensity field

(2) When the interference field strength is between −35 dBV/m and −25 dBV/m, the false alarm level increases greatly and when the interference signal is between −25 dBV/m and −15 dBV/m, the false alarm signal increases slowly

(3) When the interference field strength exceeds a certain value (−15 dBV/m), the false alarm level remains

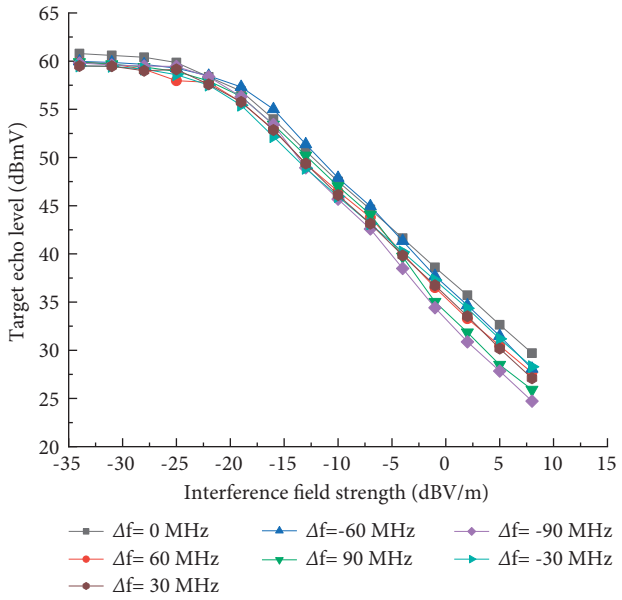

Figure 5: Relationship between the target echo level and the interference field strength.

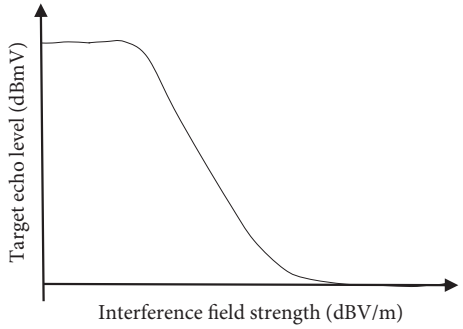

Figure 6: Theoretical target echo level curve with field intensity.

almost constant and does not change with the interference field strength

(4) When the interference frequency offset is ±90 MHz, the relationship between the false alarm level and the interference field strength is different from that of the interference frequency offset of ±30 MHz and ±60 MHz, and the false alarm level changes little with the interference field strength

Taking center frequency interference as an example, the relationship between the target echo level and false alarm level is compared as shown in Figure 9.

Figure 9 shows that firstly, when the interference signal is small, that is, the interference field strength is between −35 dBV/m and −25 dBV/m, the RF front end works in the linear region, the useful signal gain is constant, and the interference signal gain is proportional to the interference signal, which increases with the increase of the interference signal. Secondly, when the interference signal is between −25 dBV/m and −15 dBV/m, the useful signal decreases and the false alarm signal increases slowly. Thirdly, when the interference field strength is greater than −15 dBV/m, the

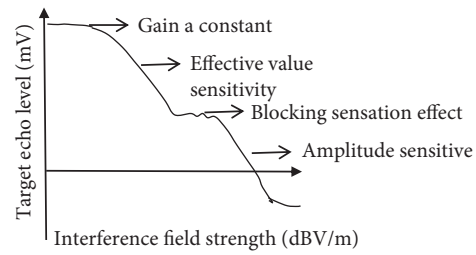

Figure 7: Theoretical target echo level curve with field intensity in linear coordinates.

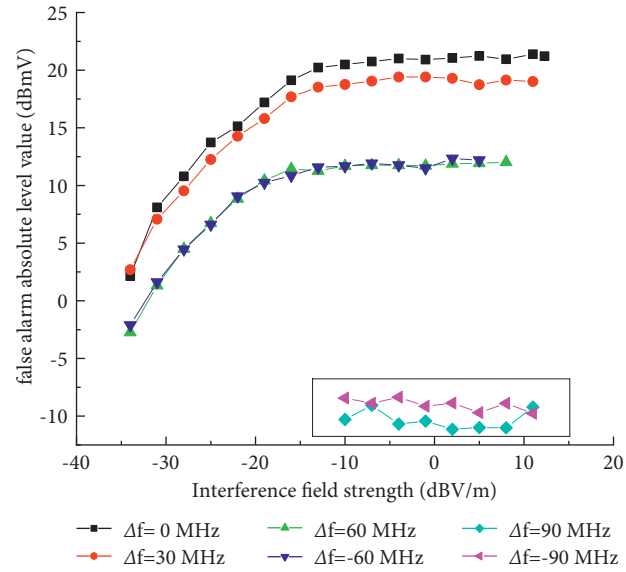

Figure 8: The relationship between the absolute value of the false alarm level and the interference field strength.

useful signal is completely blocked and the false alarm signal remains constant. In addition, under the same interference field strength, the useful signal decreases by 40 dB and the false alarm level increases by 20 dB. The experimental results are consistent with the previous theoretical analysis. Figure 9 illustrates the relationship between the false alarm interference signal and the target echo signal in the actual test process. This relationship curve actually depends on the weight before their respective coefficients. Due to the representativeness of the selected frequency points, it is inferred that the single-frequency CW-EMI effect law of the tested equipment will present a similar effect law.

3.3. Selection of Test Criteria. The law of CW electromagnetic effect of equipment is further studied, and combined with GJB151B-2013, the sensitive criterion of effect parameters was selected [30]. On the one hand, the reasonable sensitivity criterion reflects the change of equipment technical index under electromagnetic interference. On the other hand, it reflects the stability of the equipment. Combined with the single-frequency CW effect test and radar working principle, the sensitive criteria of jamming and false alarm jamming are determined [29].

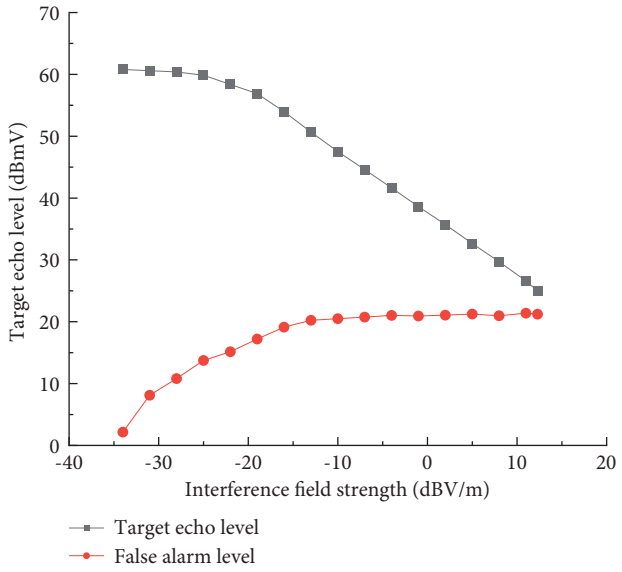

Figure 9: The relationship between useful signal echo level and false alarm interference level and interference field strength when $\Delta f = 0$ MHz.

Firstly, the sensitive criterion of blocking interference is selected reasonably. It can be seen from Figure 9 that when the interference field strength is less than −25 dBV/m, the change of echo level changes slightly, and the radar is not sensitive to the change of interference field strength. Between −25 dBV/m and −15 dBV/m, the change of echo level with the change of interference field strength is in the transition period; selecting the sensitive criterion is easy to introduce large error. When the interference field strength is greater than −15 dBV/m, the relationship between the echo level and the interference field strength is relatively certain, and the sensitive criterion for this interval is more accurate. Combined with the radar equation [31], when the useful signal is reduced by 6 dB, that is, the echo level of the radar target is suppressed by 6 dB, the maximum detection range of the radar becomes 70% of the original. After comprehensive consideration, the target echo level compressed by 6 dB is selected as the criterion of EUT jamming [29].

Secondly, the sensitivity criterion of false alarm jamming is selected. Previous formulas (7) and (8) explain the mechanism of false alarm interference. That is, the single-frequency EMI enters the RF front end of the receiver, mixes with the LO signal to generate low-frequency signal, and enters the low-pass filter to form false alarm interference. During the test, a 12-bit resolution data acquisition card is used for signal acquisition, and the range is ±5 V. After A/D conversion, the corresponding minimum digital level is $u = 20\lg(5 \times 2 \times 10^3/2^{12}) \approx 8\ dB\ mV$. In the later digital processing process, it can be considered that the resolution of the tested radar reaches half a number, and the corresponding level is $u = 20\lg(5 \times 2 \times 10^3/(2 \times 2^{12})) \approx 2\ dB\ mV$. Therefore, it can be considered that when the false alarm signal level is higher than 2 dBmV, it contains the target information; that is, the false alarm level of 2 dBmV is used as the electromagnetic sensitivity criterion of EUT false alarm interference.

3.4. Electromagnetic Interference Effect Sensitive Threshold Test. Combined with GJB8848-2016, the output of the signal generator is adjusted by the variable step size up and down until the tested radar echo level is suppressed by 6 dB, and the sensitivity threshold of radar equipment under different interference frequencies is tested. The same method is used to record the threshold of critical interference field intensity when the target level of false alarm is 2 dBmV. The single-frequency critical sensitive threshold curves of blocking jamming and false alarm jamming are shown in Figures 10 and 11, respectively.

It can be seen from Figure 10 that

(1) The radar sensitivity threshold curve of the test is roughly "U" shaped, taking the center frequency f_0 of the working signal as the center, and the sensitivity threshold curve is approximately symmetrical.

(2) The sensitive bandwidth is about $f_0 \pm 200$ MHz, which is surely wider than the working frequency f_0 of the tested radar (±100 MHz). This phenomenon is mainly related to the filter bandwidth setting behind the mixer of the radar RF front end. Third, the interference frequency offset is in the range of 130 MHz–200 MHz, that is, 130 MHz $< \Delta f <$ 200 MHz, and the critical interference field strength rises rapidly, which is in line with the performance of the RF front-end filter of the tested equipment.

(3) The closer the interference signal frequency is to the working signal frequency, the easier it is to enter the RF front end of the receiver. In other words, the smaller Δf is, the easier the radar under test is to be jammed.

(4) The right side of the band is lower than the left side of the interference threshold, and $\Delta f = +100$ MHz critical interference field intensity sensitivity threshold is the lowest, that is, −22.7 dBV/m interference field intensity can cause the test equipment to be disturbed.

(5) The interference threshold of the left side of the band is higher than that of the right side, which ranges from 0.9 dB to 3.5 dB. This phenomenon is mainly related to the signal amplification ratio of each frequency by the receiving circuit components of the RF front end of the receiver.

Under a completely ideal condition, the sensitive frequency band of the tested equipment is shown in Figure 12, and the sensitive frequency band is strictly equal to the working frequency band of the tested radar (±100 MHz).

In theory, the sensitive frequency band of the tested device should be as shown in Figure 13, considering the distribution of the internal circuit of the receiver, the performance of the filter, and the parameters of the components.

In theory, the sensitive frequency band of the tested device should be as shown in Figure 11, considering the distribution of the internal circuit of the receiver, the

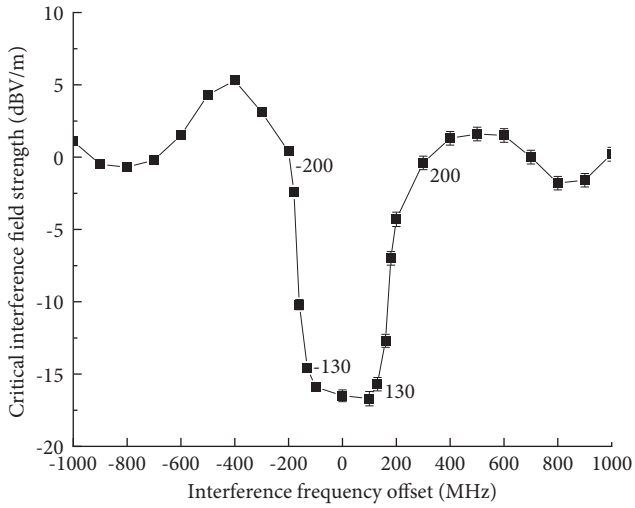

Figure 10: The blocking interference sensitivity threshold curves under different working signal intensities.

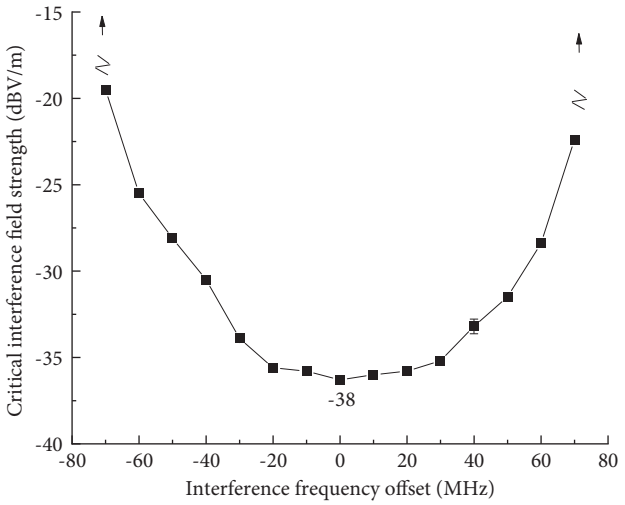

Figure 11: False alarm jamming sensitivity threshold curves under different working signal intensities.

performance of the filter, and the parameters of the components.

Using the same test method, the single-frequency critical sensitive threshold curves of false alarm jamming are obtained as shown in Figure 11.

It can be seen from Figure 11 that firstly, the electromagnetic sensitive frequency band of the radar false alarm signal is $f_0 \pm 70$ MHz, which is narrower than the working frequency band of the tested radar. Secondly, the closer the frequency of the interference signal and the working signal is, the easier the tested equipment is to be affected by external electromagnetic interference: the tested equipment is the most sensitive to the interference signal of the center frequency, that is, $\Delta f = 0$ MHz, and the minimum critical interference field is −38 dBV/m. Thirdly, with the increase of interference frequency offset, the critical interference field strength increases rapidly. Last but not least, the jamming frequency offset continues to increase. When the jamming

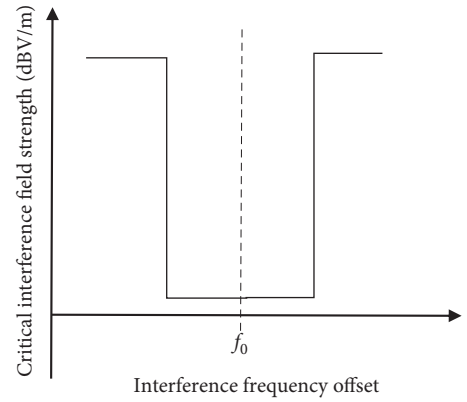

Figure 12: The device is sensitive to band curves in ideal condition.

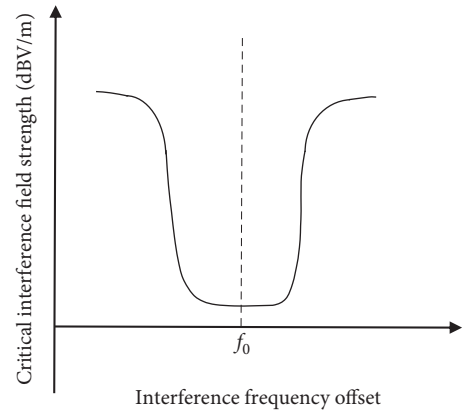

Figure 13: The device is sensitive to band curves theoretically.

frequency offset is greater than 70 MHz, it is difficult to produce effective false alarm jamming on radar.

Under ideal conditions, the receiver internal shielding is good, and interference signals cannot enter the receiver inside. In theory, the frequency band curve of device false alarm interference is similar to that shown in Figure 13. The judgment of radar false alarm interference signal is related to the number of radar data acquisition cards. Different bits may get different electromagnetic sensitivity bandwidths, but the law of electromagnetic interference effect and the thinking of analyzing problems are the same.

4. Conclusion

In this study, the influence of continuous wave electromagnetic interference on radar system performance is studied. Based on the front door coupling theory and through the nonlinear analysis of radar RF front-end circuit, the expressions of useful signal and interference signal received by radar are derived. And then the radar electromagnetic interference injection experiment is carried out to explain the experimental phenomenon and summarize the effect law. The research results lay a foundation for the evaluation of radar EMI performance in the next step.

CW electromagnetic interference not only produces suppression effect on radar echo level, but also produces

false target and makes radar appear false alarm phenomenon.

Radar echo level and false alarm level were selected as effect parameters, and the relationship between the effect parameters of blocking jamming and false alarm jamming under CW electromagnetic interference is analyzed theoretically. By using the injection equivalent test method, the EMI injection test was carried out on the tested radar, and the variation curve of radar effect parameters with the intensity of jamming field under CW electromagnetic interference was obtained. Under different jamming frequencies, the variation law of blocking jamming and false alarm jamming is the same, which indicates that the law of radar subjected to CW electromagnetic interference has a certain universal significance. Taking 6 dB and 2 dB as the electromagnetic sensitivity criteria of blocking jamming and false alarm jamming, the CW electromagnetic interference sensitivity threshold test was carried out on the tested radar. The results show that the electromagnetic sensitivity threshold curve of blocking jamming and false alarm jamming is centered on the working signal f_0, and roughly presents "*U*" shape. The closer the frequency of the interference signal and the working signal is, the easier it is to interfere with the test equipment. When the interference frequency difference is greater than 200 MHz, the interference signal will not enter the receiver along with the useful signal, and the tested radar has strong out-of-band anti-EMI capability. The difference between the two is that the range of electromagnetic sensitivity threshold curve is wider than the operating frequency band of the tested radar when the tested equipment produces blocking jamming. The electromagnetic sensitivity threshold curve of the jamming echo level presents the shape of "fluctuation oscillation," and the width of the electromagnetic sensitivity band is wider than the bandwidth of the working band of the tested equipment itself. The electromagnetic sensitivity threshold curve of false alarm level shows a "*U*" shape, and the electromagnetic sensitivity bandwidth is less than the working frequency bandwidth of the tested equipment.

Data Availability

The data used to support the findings of this study are available from the corresponding author upon request.

Conflicts of Interest

The authors declare that they have no conflicts of interest regarding the publication of this study.

Acknowledgments

This work was supported by the National Science Foundation of Hebei Province (E2019506032).

References

[1] International Electrotechnical Commission, *IEC/TS 61000-1-2 Electromagnetic Compatibility (EMC)-Methodology for the Achievement of the Functional Safety of Electrical and Electronic with Regard to Electromagnetic Phenomena*, International Electrotechnical Commission, Geneva, Switzerland, 2008.

[2] B. Qu, J. Wei, Z. Tang, T. Yan, and Z. H. Zhou, "Analysis of combined effects of multipath and CW interference on coherent delay lock loop," *Wireless Personal Communications*, vol. 77, no. 3, pp. 2213–2233, 2015.

[3] L. Wang, X. Shen, and B. Zhou, "Review on cognition of complex electromagnetic environment," *Aerospace Electronic Warfare*, vol. 36, no. 2, pp. 1–6, 2020.

[4] C. Temane, J. Makiche, and J. Nujoma, "Characterization of complex electromagnetic environment created by multiple sources of electromagnetic radiation," *International Journal of Electrical, Computer, Electronics and Communication Engineering*, vol. 8, no. 11, pp. 1650–1654, 2014.

[5] S. J. Yuan, B. Pei, Z. H. Liu, and M. F. Sun, "Testing and analysis of communication equipments mutual interference under complex electromagnetic environment," *Applied Mechanics and Materials*, vol. 557, pp. 978–981, 2014.

[6] W. Du, *Design and Implementation of Ku Band Navigation Radar System*, Beijing Institute of Technology, Beijing, China, 2019.

[7] X. Du, G. Wei, and S. Ren, "Analysis of blocking effect of single frequency continuous wave electromagnetic radiation in swept frequency radar," *Systems Engineering and Electronics*, vol. 42, no. 12, pp. 2742–2746, 2020.

[8] J. Fan, J. Hao, Z. Song, and X. Liu, "Modelling and simulation of the modified equivalent circuit of electromagnetic radiation effects," *Applied Mechanics and Materials*, vol. 475, no. 3, pp. 1661–1665, 2014.

[9] M. Guo, T. Liu, and Y. Ye, "Hybrid harmonic-intermodulation distortion behavioral model for shortwave power amplifiers," *International Journal of RF and Microwave Computer-Aided Engineering*, vol. 29, no. 7, pp. 1–5, 2019.

[10] N. Li, "Study on jamming effect of multiple false targets with radar," *Journal of Projectiles Rockets Missiles and Guidance*, vol. 40, no. 2, pp. 65–68, 2020.

[11] W. Li, F. Huang, H. Yang, and K. Wang, "Efficiency analysis of radar noise jamming and multiple false target jamming," *Journal of CAEIT*, vol. 8, no. 4, pp. 403–406, 2013.

[12] A. Balaei, A. Dempster, and P. Lo, "Characterization of the effects of CW and pulse CW interference on the GPS signal quality," *Aerospace Electronic Systems IEEE Transaction on*, vol. 45, no. 4, pp. 1418–1431, 2009.

[13] International Electrotechnical Commission, *IEC-61000-4-3 Electromagnetic Compatibility (EMC) Part 4-3: Testing and Measurement Techniques –Radiated, Radio-Frequency, Electromagnetic Field Immunity Test*, International Electrotechnical Commission, Geneva, Switzerland, 2010.

[14] Y. Wang, G. Wei, and W. Li, "Mechanism modeling and verification of receiver with in-band dual-frequency blocking jamming," *Transactions of Beijing Institute of Technology*, vol. 38, no. 7, pp. 709–714, 2018.

[15] W. Li, G. Wei, X. Pan, H. Wan, and X. Lu, "Electromagnetic compatibility prediction method under the in-band interference environment," *IEEE Transactions on Electromagnetic Compatibility*, vol. 6, no. 20, pp. 520–528, 2018.

[16] G. Wei, L. Geng, and X. Pan, "Mechanism of electromagnetic radiation effects for communication equipment," *High Voltage Engineering*, vol. 40, no. 9, pp. 2685–2692, 2014.

[17] Y. Fan, E. Cheng, and M. Wei, "Effects of CW interference on the BDS receiver and analysis of the coupling path of electromagnetic energy," *IEEE ACCESS*, vol. 7, no. 11, Article ID 155885, 2019.

[18] X. Pan, G. Wei, and X. Lu, "Test method of using differential mode injection as a substitute for high intensity electromagnetic pulse radiation," *Chinese Journal of Radio Science*, vol. 32, no. 2, pp. 151–160, 2017.

[19] B. Du, Y. Chen, W. Gao, and L. Liu, "Research on electromagnetic effect of unmanned aerial vehicle data link based on injection method," *High Voltage Engineering*, vol. 44, no. 10, pp. 3322–3327, 2018.

[20] X. Lu, G. Wei, X. Pan, X. Zhou, and L. Fan, "A pulsed differential-mode current injection method for electromagnetic pulse field susceptibility assessment of antenna systems," *IEEE Trans.on Electromagnetic Compatibility*, vol. 57, no. 6, pp. 1435–1446, 2015.

[21] Q. Zhang, *Research on Electromagnetic Interference Effect and Modeling Evaluation Method of UAV Satellite Navigation Terminal*, Shijiazhuang Campus of Army Engineering University, Shijiazhuang, China, 2021.

[22] J. B. Mazzochette, "An interference cancellation system for a hopping hf military communication network," in *Proceedings of the MILCOM 1985 -IEEE Military Communications Conference*, Boston, MA, USA, October 1985.

[23] R. Manda, P. P. Raj, and P. R. Kumar, "MMF analysis of polyphase sequences for emi suppression using cyclic algorithm-pruned," in *Proceedings of the 15th International Conference on ElectroMagnetic Interference & Compatibility (INCEMIC)*, Bengaluru, India, November 2018.

[24] M. Nazari, W. Huang, and C. Zhao, "Radio frequency interference suppression for HF surface wave radar using CEMD and temporal windowing methods," *IEEE Geoscience and Remote Sensing Letters*, vol. 17, 2018.

[25] H. Yu, N. Liu, L. Zhang et al., "An interference suppression method for multistatic radar based on noise subspace projection," *IEEE Sensors*, vol. 20, 2020.

[26] S. Ren, G. Wei, and X. Pan, "Experimental study on radiation effect of in-band continuous wave on typical radar equipment," *High Power Laser and Particle Beams*, vol. 32, no. 5, pp. 61–66, 2020.

[27] D. Zhang, Y. Chen, and H. Wan, "Prediction of electromagnetic compality for dynamic datalink of UAV," *IEEE Trasactions on Electromagnetic Compatibility*, vol. 61, no. 5, pp. 1–9, 2018.

[28] *GJB8848-2016 Electromagnetic Environmental Effects Test Methods for Systems*, Equipment Development Department of the Central Military Commission, Beijing, China, 2016.

[29] X. Du, G. Wei, K. Zhao, S. Ren, H. Zhao, and J. Zheng, "Study on electromagnetic sensitivity of ku-bandstepped frequency radar," in *Proceedings of the IEEE 13th Global Symposium on Millimeter-Waves & Terahertz (GSMM)*, Nanjing, China, May 2021.

[30] *GJB 151B-2013 Electromagnetic Emission and Susceptibility Requirements and Measurements for Military Equipment and Subsystems*, Military Standard Press of General Equipment Department, Beijing, China, 2013.

[31] E. Mao and T. Long, Y. Han, Digital signal processing of stepped frequency radar," *Acta Aeronautica et Astronautica Sinica*, vol. 22, no. S0, pp. 16–257, 2001.